NASA/CR-2001-211231
ICASE Report No. 2001-30

Analysis of Linear Parameter Varying System Models Based on Reachable Sets

Jong-Yeob Shin
ICASE, Hampton, Virginia

ICASE
NASA Langley Research Center
Hampton, Virginia

Operated by Universities Space Research Association

National Aeronautics and
Space Administration

Langley Research Center
Hampton, Virginia 23681-2199

Prepared for Langley Research Center
under Contract NAS1-97046

October 2001

ANALYSIS OF LINEAR PARAMETER VARYING SYSTEM MODELS BASED ON REACHABLE SETS

JONG-YEOB SHIN *

Abstract. This paper presents the analysis method of quasi-LPV models, comparing the ellipsoid set which contains the reachable set of a nonlinear system to define which quasi-LPV model is less conservative to represent the nonlinear dynamics. Three quasi-LPV models are constructed from a nonlinear model using three different methods, to facilitate synthesis of an LPV controller for the nonlinear system. The comparison results of closed-loop system performance with synthesized LPV controllers correspond to the analysis results of quasi-LPV models.

Key words. LPV model, reachable set, LPV control synthesis

Subject classification. Guidance and Control

1. Introduction. One of control schemes for nonlinear systems is a linear parameter varying (LPV) technique [7, 6, 11, 4, 3, 10]. This approach is particularly appealing in that nonlinear plants are treated as linear systems with varying parameters. This allows linear control techniques to be applied to nonlinear systems. In applying LPV analysis and synthesis methodology to nonlinear systems, an LPV plant model of a nonlinear system is required to describe the nonlinear dynamics. Since an LPV controller is synthesized based on an LPV model and is applied to control the nonlinear system, it is important to choose which LPV model is used for an LPV controller synthesis to lead a less conservative result.

There are three different approaches to generate an LPV model from a nonlinear mathematical model of a nonlinear system. Conventionally, an LPV model is constructed by the set of linearized models around equilibrium points. Another approach is state transformation which changes state coordinates to remove nonlinearity in the dynamics [5, 8]. The other approach is function substitution which formulates nonlinear functions into quasi-LPV form functions [15, 16, 9]. The LPV models generated by these three methods have been discussed in terms of accuracy to present a nonlinear dynamics by comparing time simulation results with the pre-defined input signals [8, 1]. Comparison of the time responses is one of approaches to decide which LPV model will be used for LPV analysis and synthesis of a nonlinear system.

There are possibilities for existence for different LPV models to produce time responses of a nonlinear system accurately within ignorable error range. Therefore, in this case, comparison of the time simulation results of the LPV models is not sufficient to analyze the models. In this paper, one of approaches is demonstrated to analyze LPV models to find which LPV model is less conservative to describe the nonlinear system.

In this paper, three different LPV models of a nonlinear system are provided by three methods and time simulation of three LPV models with the pre-defined input signals are presented. Ellipsoids which contain the reachable set of the nonlinear system are calculated according to each LPV model and compared the sizes of the ellipsoids. Also, each LPV controller is synthesized, based on each LPV model and is applied to control the nonlinear system.

*ICASE, MS. 132c, NASA Langley Research Center, Hampton, VA, 23681 (email:j.y.shin@larc.nasa.gov). This research was supported by the National Aeronautics and Space Administration under NASA Contract No. NAS1-97046 while the author was in residence at ICASE, NASA Langley Research Center, Hampton, VA 23681-0001

Outline of this paper is follows. In section 2, conventional LPV control synthesis used in this paper is briefly summarized. In section 3, an analysis methodology of quasi-LPV models is presented, calculating an ellipsoid which contains a reachable set. In section 4, an example of analysis of quasi-LPV models is demonstrated and also nonlinear simulations with LPV controllers synthesized based on each quasi-LPV model are presented for comparison. This paper concludes with a brief summary in section 5.

2. LPV Control Synthesis. In this section, a quasi-LPV system is defined and an LPV control synthesis methodology is briefly described. Consider a generalized linear open-loop system as functions of parameters $\rho(t) \in \mathcal{P}$. For a compact subset $\mathcal{P} \subset \mathcal{R}^s$, the parameter variation set denotes the set of all piecewise continuous functions mapping R (time) into $\mathcal{P}$ with a finite number of discontinuities in any interval, where s is number of parameters. An LPV open-loop system can be written as

$$\begin{bmatrix} \dot{x}(t) \\ e(t) \\ y(t) \end{bmatrix} = \begin{bmatrix} A(\rho(t)) & B_1(\rho(t)) & B_2(\rho(t)) \\ C_1(\rho(t)) & 0 & D_{12}(\rho(t)) \\ C_2(\rho(t)) & D_{21}(\rho(t)) & 0 \end{bmatrix} \begin{bmatrix} x(t) \\ d(t) \\ u(t) \end{bmatrix} \tag{2.1}$$

where $y(t)$, $e(t)$, $d(t)$ and $u(t)$ are measurements, errors, disturbances, and control signals. A quasi-LPV system is defined when scheduling parameter vector ρ contains part of state vector as $[x_1 \;\; \rho_e]$, where ρ_e is an exogenous scheduling parameter vector and the state vector $x = [x_1 \;\; x_2]$. Hereafter, ρ denotes $\rho(t)$. The induced $\mathcal{L}_2$ norm of d to e is defined as

$$\sup_{\rho \in \mathcal{P}, d \in \mathcal{L}_2, ||d||_2 \neq 0} \frac{||e||_2}{||d||_2}.$$

In an LPV synthesis methodology, suppose there is an LPV output feedback controller $K(\rho)$ which stabilizes the closed-loop system exponentially and makes the induced $\mathcal{L}_2$-norm of d to e less than γ. The controller $K(\rho)$ can be written as

$$\begin{bmatrix} \dot{x}_k \\ u \end{bmatrix} = \begin{bmatrix} A_k(\rho) & B_k(\rho) \\ C_k(\rho) & D_k(\rho) \end{bmatrix} \begin{bmatrix} x_k \\ y \end{bmatrix}. \tag{2.2}$$

An LPV controller $K(\rho)$ can be constructed from solutions of $X \in \mathcal{R}^{n \times n}$ and $Y \in \mathcal{R}^{n \times n}$ of the following optimization problem [4].

$$\min_{X, Y \in \mathcal{R}^{n \times n}} \gamma \tag{2.3}$$

subject to

$$\begin{bmatrix} X\hat{A}^T(\rho) + \hat{A}(\rho)X - B_2(\rho)B_2^T(\rho) & XC_{11}^T(\rho) & \gamma^{-1}B_1(\rho) \\ C_{11}(\rho)X & -I_{n_{e_1}} & 0 \\ \gamma^{-1}B_1^T(\rho) & 0 & -I_{n_d} \end{bmatrix} < 0 \tag{2.4}$$

$$\begin{bmatrix} \tilde{A}(\rho)Y + Y\tilde{A}^T(\rho) - C_2^T(\rho)C_2(\rho) & YB_{11}(\rho) & \gamma^{-1}C_1^T(\rho) \\ B_{11}^T(\rho)Y & -I_{n_{d_1}} & 0 \\ \gamma^{-1}C_1(\rho) & 0 & -I_{n_e} \end{bmatrix} < 0, \tag{2.5}$$

$$\begin{bmatrix} X & \gamma^{-1}I_n \\ \gamma^{-1}I_n & Y \end{bmatrix} \geq 0, \tag{2.6}$$

$$X > 0, \;\; Y > 0$$

where

$$\hat{A}(\rho) \equiv A(\rho) - B_2(\rho)C_{12}(\rho), \;\; \tilde{A}(\rho) \equiv A(\rho) - B_{12}(\rho)C_2(\rho), \tag{2.7}$$

and n is number of states of the generalized open-loop system. Note that X and Y are constant positive definite matrices.

A method to construct an LPV controller $K(\rho)$ from the solution matrix X and Y of the LMI optimization problem is taken from Ref.[4]. An LPV controller is constructed as[4]:

$$A_k(\rho) = A(\rho) + B_2(\rho)F(\rho) + Q^{-1}YL(\rho)C_2(\rho) - \gamma^{-2}Q^{-1}M(\rho), \tag{2.8}$$

$$B_k(\rho) = -Q^{-1}YL(\rho), \tag{2.9}$$

$$C_k(\rho) = F(\rho), \tag{2.10}$$

$$D_k(\rho) = 0 \tag{2.11}$$

where matrices Q, $F(\rho)$, $L(\rho)$, and $M(\rho)$ are defined as

$$\begin{aligned} Q &= Y - \gamma^{-2}X^{-1}, \\ F(\rho) &= -[B_2^T(\rho)X^{-1} + D_{12}^T(\rho)C_1(\rho)], \\ L(\rho) &= -[Y^{-1}C_2^T(\rho) + B_1(\rho)D_{21}^T(\rho)], \\ M(\rho) &= H(\rho) + \gamma^2 Q[-Q^{-1}YL(\rho)D_{21}(\rho) - B_1(\rho)]B_1^T(\rho)X^{-1}. \end{aligned}$$

Matrix $H(\rho)$ is defined as

$$H(\rho) = -[X^{-1}A_F(\rho) + A_F(\rho)^T X^{-1} + C_F^T(\rho)C_F(\rho) + \gamma^{-2}X^{-1}B_1(\rho)B_1(\rho)^T X^{-1}]$$

with $A_F(\rho) = A(\rho) + B_2(\rho)F(\rho)$ and $C_F(\rho) = C_1 + D_{12}F(\rho)$. The closed-loop system with the controller $K(\rho)$ is exponentially stable and the induced $\mathcal{L}_2$ norm is less than γ. The proof can be found in Ref. [4]. To make the optimization problem of equation (2.3) computationally tractable, scheduling parameters ρ are discretized into grid points. Thus, infinite LMI constraints, equations (2.4)-(2.5), are presented as finite number of LMI constraints. Note that the LPV controller may be different based on scheduling-parameter grid points.

Note that the open-loop LPV system matrices $A(\rho)$, $B(\rho)$, $C(\rho)$ and $D(\rho)$ are used to construct the LPV controller (see equations (2.8)-(2.11)). The LPV controller can be different based on the different LPV models of a nonlinear system, even if the different LPV models can produce the exact same input-output time responses for each other.

3. Analysis of Quasi-LPV Model. In this section, one of approaches to analyze an LPV model is presented in terms of the sizes of ellipsoids which contain a reachable set of a nonlinear system. Before we introduce an analysis method of LPV models of a nonlinear system, a class of nonlinear systems used in this paper is defined as follows.

Consider a nonlinear system in which an input vector enters affinely. A nonlinear system can be written as

$$\dot{x} = F(x) + B(x)u \tag{3.1}$$

where a state vector x is in $\mathcal{R}^n$, an input vector u is in $\mathcal{R}^m$, continuous function $F(x) : \mathcal{R}^n \to \mathcal{R}^n$ and $B(x) : \mathcal{R}^n \to \mathcal{R}^{n\times m}$. The reachable set of a nonlinear system with bounded-energy inputs is defined by

$$\mathcal{R}_{nl} \equiv \left\{ x(T) \;\middle|\; \dot{x} = F(x) + B(x)u,\;\; x(0) = 0,\;\; \int_0^T u^T u dt \le \alpha^2,\;\; T \ge 0 \right\} \tag{3.2}$$

where α is a given positive constant. The reachable set of a nonlinear system is bounded. Here an initial point of x is defined as 0 without loss of generality. Definition of an invariant set used in this paper is follows:

Definition 3.1 *Invariant set*
Let a set ε denote a set centered at the origin

$$\varepsilon = \{x \in \mathcal{R}^n | V(x) < 1\}.$$

The set ε is said to be invariant if for every trajectory $x(t)$ of a nonlinear system, $x(0) \in \varepsilon$ implies $x(t) \in \varepsilon$ for all t. A function $V(x)$ is a Lyapunov function.

It is easily shown that when $V(x) > 0$ and $\frac{dV(x)}{dt} < 0$ for all trajectory satisfying the nonlinear dynamics in equation (3.1), the set ε is invariant.

A quasi-LPV model of a nonlinear system can be produced with or without a bounded uncertainty block to capture nonlinear dynamics.

- Case 1 : a quasi-LPV model can describe the nonlinear dynamic model without an uncertainty block. A quasi-LPV model is

$$\dot{x} = A(x)x + B(x)u = F(x) + B(x)u. \tag{3.3}$$

  The reachable set of a quasi-LPV model is defined as

$$\mathcal{R}_{be} \equiv \left\{ x \;\middle|\; \dot{x} = A(x)x + B(x)u,\;\; x(0) = 0,\;\; \int_0^T u^T u dt \le \alpha^2,\;\; T \ge 0 \right\}. \tag{3.4}$$

  Thus, it is obvious that the reachable set $\mathcal{R}_{be}$ is equal to $\mathcal{R}_{nl}$.

- Case 2: a quasi-LPV model can describe the nonlinear dynamic model with a bounded uncertainty block. A quasi-LPV model is

$$\dot{x} = A(x)x + B_u(x)u + B_w(x)w, \tag{3.5}$$
$$z = C_z(x)x + D_{zu}(x)u + D_{zw}(x)w, \tag{3.6}$$
$$w = \Delta z \tag{3.7}$$

  where $B_w(x) \in \mathcal{R}^{n\times p}$, $w \in \mathcal{R}^p$, $C_z \in R^{q\times n}$, $D_{zu} \in \mathcal{R}^{q\times m}$, $D_{zw} \in \mathcal{R}^{q\times p}$, and $||\Delta|| \le \beta$. The reachable set of a quasi-LPV model is defined as

$$\mathcal{R}_{beu} \equiv \left\{ x \;\middle|\; \begin{array}{ll} \dot{x} & = A(x)x + B(x)u + B_w(x)w, \\ z & = C_z(x)x + D_{zu}(x)u + D_{zw}(x)w, \quad x(0) = 0, \;\; \int_0^T u^T u dt \le \alpha^2, \;\; T \ge 0 \\ w & = \Delta z \end{array} \right\}. \tag{3.8}$$

  Assume that there exists Δ such that

$$\mathcal{R}_{nl} \subset \mathcal{R}_{beu}. \tag{3.9}$$

Note that calculating the size and structure of Δ to validate equation (3.9) is out of this paper scope.

Suppose there exists a Lyapunov function V such that

$$\frac{dV(x(t))}{dt} \leq \frac{1}{\alpha^2}||u(t)||_2^2 \tag{3.10}$$

for every $x(t)$ and $u(t)$ satisfying equation (3.3) or equations (3.5)-(3.7). Then there exists the invariant set $\{x \mid V(x) < 1\}$ which contains the reachable set $\mathcal{R}_{be}$ or $\mathcal{R}_{beu}$, according to each quasi-LPV model.

3.1. Singular Quadratic Lyapunov Function. In this section, an LMI optimization problem is formulated to calculate the smallest ellipsoid which contains the reachable set, using a singular quadratic Lyapunov function $V(x) = x^T P x$. For the two cases: Case 1 and Case 2, the LMI optimization problems are formulated as follows.

For case 1:

$$\sup_{P \in \mathcal{R}^{n \times n}} Tr(P) \tag{3.11}$$

subject to

$$\begin{bmatrix} A(x)^T P + PA(x) & PB(x) \\ B(x)^T P & -\frac{1}{\alpha^2} I \end{bmatrix} < 0. \tag{3.12}$$

The LMI constraint of equation (3.12) is easily derived from $\frac{dV(x(t))}{dt} \leq \frac{1}{\alpha^2}||u(t)||_2^2$ and equation (3.3). Thus, the set $\{x(t)|x(t)^T P x(t) < 1, t > T\}$ contains the reachable set $\mathcal{R}_{be}$. Also, it is noticed from the LMI constraint that the ellipsoid is an invariant set.

For case 2:

$$\sup_{P} Tr(P) \tag{3.13}$$

$$\begin{bmatrix} A^T(x)P + PA(x) + tC_z^T(x)C_z(x) & PB_u(x) + tC_z^T(x)D_{zu}(x) & PB_w(x) + tC_z^T(x)D_{zw}(x) \\ B_u^T(x)P + tD_{zu}^T(x)C_z(x) & -\frac{1}{\alpha^2}I + tD_{zu}^T(x)D_{zu}(x) & 0 \\ B_w^T(x)P + tD_{zw}^T(x)C_z(x) & 0 & tD_{zw}^T(x)D_{zw}(x) - \frac{t}{\beta^2}I \end{bmatrix} < 0 \tag{3.14}$$

$$P > 0, \quad t \geq 0 \tag{3.15}$$

where $||\Delta|| \leq \beta$ and β is given constant. The LMI constraint of equation (3.14) is easily derived from $\frac{dV(x(t))}{dt} \leq \frac{1}{\alpha^2}||u(t)||_2^2$ and equations (3.5)-(3.7), using $\mathcal{S}$-procedure [14]. The set $\{x(t)|x(t)^T P x(t) < 1, t > T\}$ contain the reachable set $\mathcal{R}_{beu}$. Also, it is noticed from the LMI constraint that the ellipsoid is an invariant set.

The size of the ellipsoid is defined as

$$S_P = C \prod_i^n \lambda_i(P) \tag{3.16}$$

where C is constant which is dependent on the geometry of the ellipsoid. Thus, it is easy to compare the size of the ellipsoid set $\{x|x^T P x < 1\}$.

3.2. Parameter Dependent Lyapunov Function. In this section, the LMI optimization problem is formulated with the parameter-dependent Lyapunov function $V(x) = x^T P(x)x$. LMI constraints are written for each case in the same manner of formulation of LMI constraints in equations (3.12) and (3.14).

For case 1:

$$\sup_{P(x):\mathcal{R}^n \to \mathcal{R}^{n\times n}} Tr(P(x)) \tag{3.17}$$

subject to

$$\begin{bmatrix} A(x)^T P(x) + PA(x) + \dot{P}(x) & P(x)B(x)) \\ B(x)^T P(x) & -\frac{1}{\alpha^2} I \end{bmatrix} < 0. \tag{3.18}$$

For case 2:

$$\sup_{P(x):\mathcal{R}^n \to \mathcal{R}^{n\times n}} Tr(P(x)) \tag{3.19}$$

$$\begin{bmatrix} A^T(x)P(x) + P(x)A(x) + tC_z^T(x)C_z(x) + \dot{P}(x) & P(x)B_u(x) + tC_z^T(x)D_{zu}(x) & P(x)B_w(x) + tC_z^T(x)D_{zw}(x) \\ B_u^T(x)P(x) + tD_{zu}^T(x)C_z(x) & -\frac{1}{\alpha^2} I + tD_{zu}^T(x)D_{zu}(x) & 0 \\ B_w^T(x)P(x) + tD_{zw}^T(x)C_z(x) & 0 & tD_{zw}^T(x)D_{zw}(x) - \frac{t}{\beta^2} I \end{bmatrix} \leq 0 \tag{3.20}$$

$$P > 0, \quad t \geq 0. \tag{3.21}$$

Using the LMI optimization, the smallest ellipsoid to capture the reachable set of the nonlinear dynamics can be calculated. To solve the LMI optimization problem, the basis functions of $P(x)$ are required. The details of solving the LMI with $\dot{P}(x)$ will be explained in the next section. Note that the size of the set $\{x | x(t)^T P(x(t))x(t) < 1\}$ is not easy to calculate since it is not ellipsoid.

4. Example. In this section, LPV models of a nonlinear system are generated by three different methods (Jacobian linearization, state transformation, and function substitution) and each LPV model is simulated with pre-defined input signals. The simulation results are compared with nonlinear simulation results to notice that quasi-LPV models can capture the nonlinear dynamics. Also, the size of an ellipsoid which contains the reachable set of the nonlinear system is calculated for each LPV model. An LPV controller is synthesized based on each LPV model, respectively and is simulated with nonlinear system to compare the closed-loop performance.

A nonlinear system taken from Ref. [2] is

$$\begin{bmatrix} \dot{x}_1 \\ \dot{x}_2 \end{bmatrix} = \begin{bmatrix} -x_1 \\ x_1 - |x_2|x_2 - 10 \end{bmatrix} + \begin{bmatrix} 1 \\ 0 \end{bmatrix} u, \quad y = x_2. \tag{4.1}$$

It is noted that systems with similar types of nonlinearity are frequently encounted in practice [2, 13].

4.1. Quasi-LPV Models. Using Jacobian linearization around trim points, the set of linearized models can present a quasi- LPV model of the nonlinear system. The linearized model at a trim point is

$$\begin{bmatrix} \delta\dot{x}_1 \\ \delta\dot{x}_2 \end{bmatrix} = \begin{bmatrix} -1 & 0 \\ 1 & -2|x_{2_0}| \end{bmatrix} \begin{bmatrix} \delta x_1 \\ \delta x_2 \end{bmatrix} + \begin{bmatrix} 1 \\ 0 \end{bmatrix} \delta u, \quad \delta y = \delta x_2, \tag{4.2}$$

where $\delta x_1 = x_1 - x_{1_0}$, $\delta x_2 = x_2 - x_{2_0}$, $\delta u = u - u_0$, and $\delta y = y - y_0$. The associated quasi-LPV system is

$$\begin{bmatrix} \dot{\eta}_1 \\ \dot{\eta}_2 \end{bmatrix} = \begin{bmatrix} -1 & 0 \\ 1 & -2z \end{bmatrix} \begin{bmatrix} \eta_1 \\ \eta_2 \end{bmatrix} + \begin{bmatrix} 1 \\ 0 \end{bmatrix} u, \quad y = \begin{bmatrix} 0 & 1 \end{bmatrix} \begin{bmatrix} \eta_1 \\ \eta_2 \end{bmatrix} \tag{4.3}$$

where the range of $z = |x_{2_0}|$ is defined arbitrary from 0 to 5. It is noted that states, η_1 and η_2, are defined as deviation from each trim point (x_{1_0}, x_{2_0}, u_0). Thus, when scheduling parameter z changes the definitions of states of the LPV model are changed.

To use function substitution [15, 16, 9], the nonlinear system is rewritten as

$$\begin{bmatrix} \dot{\tilde{x}}_1 \\ \dot{\tilde{x}}_2 \end{bmatrix} = \begin{bmatrix} -1 & 0 \\ 1 & 0 \end{bmatrix} \begin{bmatrix} \tilde{x}_1 \\ \tilde{x}_2 \end{bmatrix} + \begin{bmatrix} 1 \\ 0 \end{bmatrix} \tilde{u} + \begin{bmatrix} -x_{1_0} + u_0 \\ x_{1_0} - |\tilde{x}_2 + x_{2_0}|(\tilde{x}_2 + x_{2_0}) - 10 \end{bmatrix} \tag{4.4}$$

where

$$\tilde{x}_1 = x_1 - x_{1_0}, \quad \tilde{x}_2 = x_2 - x_{2_0}, \quad \tilde{u} = u - u_0. \tag{4.5}$$

The nonlinearity in equation (4.4) is substituted for a function in quasi-LPV form.

$$f(\tilde{x}_2) = \begin{cases} [|x_{2_0}|x_{2_0} - |\tilde{x}_2 + x_{2_0}|(\tilde{x}_2 + x_{2_0})]/\tilde{x}_2, & \tilde{x}_2 \neq 0, \\ 0, & \tilde{x}_2 = 0. \end{cases} \tag{4.6}$$

A quasi-LPV model is written as

$$\begin{bmatrix} \dot{\tilde{x}}_1 \\ \dot{\tilde{x}}_2 \end{bmatrix} = \begin{bmatrix} -1 & 0 \\ 1 & f(\tilde{x}_2) \end{bmatrix} \begin{bmatrix} \tilde{x}_1 \\ \tilde{x}_2 \end{bmatrix} + \begin{bmatrix} 1 \\ 0 \end{bmatrix} \tilde{u}. \tag{4.7}$$

Here, a trim point is set as $(x_{1_0}, \ x_{2_0}) = (11, \ 1)$. Note that the definition of states of this quasi-LPV model is deviation from the trim point. Also, the definition of states does not change as a scheduling parameter $\tilde{x}_2$ changes.

A quasi-LPV model of the nonlinear system can be generated by changing state coordinates [5]

$$\eta_1 = x_1 - x_{1_0}(x_2), \tag{4.8}$$

$$\eta_2 = x_2 \tag{4.9}$$

where

$$x_{1_0}(x_2) = |x_2|x_2 + 10. \tag{4.10}$$

A quasi-LPV model is

$$\begin{bmatrix} \dot{\eta}_1 \\ \dot{\eta}_2 \end{bmatrix} = \begin{bmatrix} -1 - 2|\eta_2| & 0 \\ 1 & 0 \end{bmatrix} \begin{bmatrix} \eta_1 \\ \eta_2 \end{bmatrix} + \begin{bmatrix} 1 \\ 0 \end{bmatrix} r \tag{4.11}$$

where $r = u - u_0(x_2)$. Note that definition of control input r and state η_1 are changed as scheduling parameters vary. When the quasi-LPV model is simulated, the variations of $u_0(x_2)$ and η_1 should be compensated as the scheduling parameter x_2 changes.

4.2. Quasi-LPV Model Simulations. There are three quasi-LPV models to describe the nonlinear system. To compare the simulation results between the nonlinear system and the quasi-LPV model, a performance index J is introduced as $\mathcal{L}_2$ norm of error in finite time T,

$$J = \int_0^T e(t)^t e(t) \ dt = \int_0^T (y_{nl}(t) - y_{LPV}(t))^t (y_{nl}(t) - y_{LPV}(t)) \ dt \tag{4.12}$$

where y_{nl} and y_{LPV} are measurements of the nonlinear system and the quasi-LPV model, respectively. Here, T is set as 30 sec in this example.

The quasi-LPV models are simulated for the two different input signal sets (see Figure 5.1), respectively. The simulation results in Figure 5.2 show that the quasi-LPV models present the nonlinear dynamics very accurately. The differences of time responses between the quasi-LPV models and the nonlinear system are not noticeable in Figure 5.2. The performance index, J, for all quasi-LPV models is less than 10^{-7} for both different input cases. The indexes, NL, Q-LPV$_J$, Q-LPV$_s$, and Q-LPV$_f$, in Figure 5.2 are denoted as the nonlinear system, the quasi-LPV model by Jacobian linearization, the quasi-LPV model by state-transformation, and the quasi-LPV model by function substitution. Note that all quasi-LPV models can present all state dynamics of the nonlinear system very accurately. Therefore, comparing performance index is not sufficient to choose which quasi-LPV model will be used for LPV controller synthesis.

4.3. Reachable Set. In this section, the smallest ellipsoid which contains the reachable set of the nonlinear model is calculated for each quasi-LPV model.

4.3.1. Singular Quadratic Lyapunov Function. Assume a Lyapunov function $V(x) = x^T P x$, $P \in \mathcal{R}^{n \times n}$ is used to calculate the smallest set $\{x | x^T P x < 1\}$ which contains the reachable set of the nonlinear system. Consider a quasi-LPV model without an uncertainty block, which can capture the nonlinear dynamics (Case 1). To make the LMI optimization problem in equation (3.11) computationally tractable, the infinite number of LMI constraints are converted into the finite number of LMI constraints defined each grid points over the parameter space. The grid points in this example are defined as

$$x_{2_i} \in \{0.1, 0.5, 0.9, 2, 3, 4, 5\}. \tag{4.13}$$

Also, bounded energy inputs are required to solve the LMI optimization problems. Hereafter, the bounded energy inputs are defined $\int_0^T u^t u \leq 0.2$ in this example.

The solution matrix P of the LMI optimization problem is calculated, based on the quasi-LPV models generated by Jacobian linearization and function substitution, respectively. The ellipsoids corresponding to the solution matrix P are shown in Figure 5.3 for each quasi-LPV model. In Figure 5.3, possible trajectories of the nonlinear system with pre-defined several input signals bounded by constant energy are also plotted as dashed lines. It is observable that the two ellipsoids capture the candidate trajectories to represent the reachable set of the nonlinear system. Also, it is noticeable that the size of the ellipsoid based on the function substitution quasi-LPV model (Q-LPV_f) is smaller than that of the Jacobian linearization quasi-LPV model (Q-LPV_J). Thus, the quasi-LPV model generated by function substitution is less conservative than the quasi-LPV model generated by Jacobian linearization to contain the reachable set of the nonlinear system.

Since one of eigenvalues of the quasi-LPV model generated by state transformation is 0 for all grid points, it is not computationally tractable to calculate the size of the ellipsoid to contain the reachable set. It is noticeable that the quasi-LPV model can not satisfy one of the conventional assumptions for $\mathcal{H}_\infty$ and LPV synthesis [4] :

$$\begin{bmatrix} a & b1 \\ c2 & d21 \end{bmatrix} \text{ have full row rank.} \tag{4.14}$$

Thus, this analysis method can not apply for a quasi-LPV model which has zero eigenvalue over all grid points. Hereafter, we discuss two quasi-LPV models generated by Jacobian linearization and function substitution methods.

Consider that a quasi-LPV model with an uncertainty block to represent the nonlinear dynamics (Case 2). Here, unmodeled dynamics is assumed as an input multiplicative uncertainty in Figure 5.4. The uncertainty

weighting function W_n is assumed as

$$W_n = 0.0045\frac{s/0.09+1}{s/80+1}. \tag{4.15}$$

The magnitude of the uncertainty block $|\Delta|$ is bounded by one. The ellipsoids to contain the reachable set are calculated based on quasi-LPV models (Q-LPV_j and Q-LPV_f) and shown in Figure 5.5. It is noticed that the function-substitution quasi-LPV model has smaller ellipsoid to represent the reachable set than the Jacobian-linearization quasi-LPV model. Recall that the state x_2 is measurement for design an output feedback LPV controller. It is noticeable that the axis of the ellipsoid at x_2 direction is smaller of the function-substitute quasi-LPV model than the Jacobian-linearization quasi-LPV model. The set of $\{(x_1, x_2)|x^T P x < 1\}$ in Figure 5.5 is much larger than the set shown in Figure 5.3 for each quasi-LPV model, respectively. It is obvious that adding unmodel dynamics in the quasi-LPV model enlarges the size of the set $\{(x_1, x_2)|x^T P x < 1\}$. The state x_3 of augmented open-loop system is the state of the weighting function. The sizes of the ellipsoids in x_3 direction are similar to each other, based on each quasi-LPV model (Q-LPV_j and Q-LPV_f).

In this example, adding unmodel dynamics in quasi-LPV models does not change the comparison result that the function-substitution quasi-LPV model is less conservative to present the nonlinear dynamics than the Jacobian-linearization quasi-LPV model. Note that it is unknown that adding an uncertainty block changes the comparison results in general.

4.3.2. Parameter-Dependent Lyapunov Function. A Lyapunov function $V(x) = x^T P(x) x$ is used to calculate the smallest set $\{x|V(x) < 1\}$ which contains the reachable set of the nonlinear dynamics. Consider quasi-LPV models without an uncertainty block. To solve the LMI optimization problem in equation (3.17), basis functions of $P(x)$ are required. A matrix function $P(x)$ and the time derivative of $P(x)$ can be written as:

$$P(x) = \sum_{i=1}^{N} f_i(x) P_i, \quad P_i \in \mathcal{R}^{n\times n} \tag{4.16}$$

$$\dot{P}(x) = \sum_{j=1}^{s} (\sum_{i=1}^{N} \dot{x}_j \frac{\partial f_i(x)}{\partial x_j} P_i) \tag{4.17}$$

with given basis functions $f_i(x)$, where s and N are number of scheduling parameter and number of basis functions, respectively. In the example, the set of basis function $\{f_i(x)\}$ is defined as the first order polynomial function set $\{1, x_2\}$ for computational convenience. The time derivative of $P(x)$ is written as:

$$\dot{P}(x) = \dot{x}_2 P_2 \tag{4.18}$$

where $P_2 \in \mathcal{R}^{n\times n}$. In conventional parameter-dependent Lyapunov function LPV synthesis [3], constant bounded values ν of the parameter rates are used to describe the time derivative of $P(x)$ as:

$$\dot{P}(x) = \sum_{j=1}^{n} (\sum_{i=1}^{N} \pm\nu_j \frac{\partial f_i(x)}{\partial x_j} P_i), \quad |\dot{x}_j| < \nu_j \tag{4.19}$$

where $\pm\nu_j$ represents all possible combination set of $-\nu_j$ and ν_j. In this paper, the time derivative of $P(x)$ is written as

$$\dot{P}(x) = \sum_{j=1}^{n} (\sum_{i=1}^{N} \pm g_j(x) \frac{\partial f_i(x)}{\partial x_j} P_i), \tag{4.20}$$

where $g_j(x) : \mathcal{R}^n \to \mathcal{R}$ is satisfied with $|\dot{x}_j| < g_j(x)$. To evaluate equation (4.20), the function $g_j(x)$ is estimated from nonlinear dynamic simulation results with the bounded energy inputs. For this example,

$$g(x_2) = (1 + f(\tilde{x}_2))x_2 \tag{4.21}$$

where $f(\tilde{x}_2)$ is defined in equation (4.6).

The boundary of the set $\{x|x^T P(x)x < 1\}$ to contain the reachable set $\mathcal{R}_{be}$ is shown in Figure 5.6. The solid line in Figure 5.6 represents the boundary of the set $\{x|x^T P(x)x < 1\}$ calculated based on the function-substitution quasi-LPV model. The dotted line in Figure 5.6 represents the ellipsoid calculated using the singular quadratic Lyapunov function based on the function-substitution quasi-LPV model. It is noted that the set $\{x|V(x) < 1\}$ using the parameter-dependent Lyapunov function is smaller than using singular quadratic Lyapunov function. This result corresponds to that LPV control synthesis methodology using the parameter-dependent Lyapunov function leads a less conservative result than using the singular quadratic Lyapunov function [3]. The dashed-dot line in Figure 5.6 represents the set $\{x|x^T P(x)x < 1\}$ calculated based on the Jacobian-linearization quasi-LPV model. It is observed that the function-substitution quasi-LPV model is less conservative than the Jacobian-linearization quasi-LPV model to present the reachable set of nonlinear system. The analysis of quasi-LPV models with an uncertainty block leads the same result that the function-substitution quasi-LPV model is less conservative. The plots of the calculated sets are omitted for space limitation.

4.4. LPV Controller Synthesis. An LPV controller is synthesized based on each quasi-LPV model and is simulated with the nonlinear simulation to compare the closed-loop system performance.

The prime objective of an LPV control synthesis is to track a given command. An LPV controller synthesis formulation is taken from Ref. [2] shown in Figure 5.7. The performance weighting function W_1 and control weighting function W_2 are taken from Ref. [2] as

$$W_1 = \frac{0.5}{s + 0.002}, \quad W_2 = \frac{0.1s}{s + 1000}. \tag{4.22}$$

The noise weight function is defined as constant 0.05 over all frequency range to present 5% measurement error.

To solve the LMI optimization of LPV controller synthesis, a scheduling parameter is discretized over all spaces. The grid points are presented in equation (4.13). The LPV controllers are synthesized for each quasi-LPV model with same weight functions, using standard software from the MATLAB LMI toolbox [12]. There are two generated LPV controllers (Q-LPV_J, Q-LPV_f) according to two quasi-LPV models.

The responses to step change in command from -1 to 5 of the closed-loop system are shown in Figure 5.8. It is observable that the overshooting responses of the LPV controller synthesized based on the function substitution quasi-LPV model are smaller than those with the Jacobian-linearization quasi-LPV model. The calculated γ in equation (2.3) is 0.92 for the Jacobian linearization quasi-LPV model and 0.73 for the function substitution quasi-LPV model.

The performance results are correspond to the analysis results of LPV models. The ellipsoid based on the functional substitution quasi-LPV model to present a reachable set of the nonlinear system is smaller. That implies that the quasi-LPV model generated by the function substitution is less conservative. Note that it is not known that the function substitution method can always generate a less conservative quasi-LPV model in terms of an ellipsoid which contains the reachable set.

5. Conclusion. In this paper, one of approaches to compare quasi-LPV models which represent a nonlinear system is demonstrated in terms of the smallest set which contains the reachable set of the nonlinear system. Based on the size of the set, it is possible to define which quasi-LPV model is less conservative to present the reachable set. The quasi-LPV models of a nonlinear system are generated by three different methods (Jacobian linearization, state transformation, and function substitution) to facilitate to design an LPV controller of the nonlinear system. LPV controllers are synthesized based on each quasi-LPV model and simulated with the nonlinear system to compare the closed-loop performance. The performance results correspond to the results of comparing the size of the set calculated based on each quasi-LPV model. Based on the analysis results of quasi-LPV models, it is possible to choose which LPV model is used for LPV controller synthesis of a nonlinear system.

Acknowledgements. The technical monitor for this work was Dr. Christine Belcastro at NASA Langley Research Center.

REFERENCES

[1] A. Marcos and G. Balas, *Linear Parameter Varying Modeling of the Boeing 747-100/200 Longitudinal Motion*, in AIAA Guidance, Navigation and Control Conference, AIAA-01-4347, Montreal, Canada, Aug. 2001, American Institute of Aeronautics and Astronautics.

[2] D.J. Leith and W.E. Leithead, *Counter-Example to a common LPV Gain-Scheduling Design Approach*, tech. report, Industrial Control Center, University of Strathclyde, UK, 1999.

[3] F. Wu, *Control of Linear Parameter Varying Systems*, PhD thesis, Department of Mechanical Engineering, University of California, Berkeley, 1995.

[4] G. Becker, *Quadratic Stability and Performance of Linear Parameter Dependent Systems*, PhD thesis, Department of Engineering, University of California, Berkeley, 1993.

[5] J. Shamma, *Gain-Scheduled Missile Autopilot Design Using Linear Parameter Varying Transformations*, Journal of Guidance, Control, and Dynamics, 16 (1993), pp. 256–261.

[6] J. Shamma and M. Athans, *Analysis of Gain Scheduled Control for Nonlinear Plants*, IEEE Transactions on Automatic Control, 35 (1990), pp. 898–907.

[7] ——, *Guaranteed Properties of Gain Scheduled Control for Linear Parameter-Varying Plants*, Automatica, 35 (1991), pp. 559–564.

[8] J-Y. Shin, *Worst-case Analysis and Linear Parameter Varying Control of Aerospace System*, PhD thesis, University of Minnesota, 2000.

[9] J-Y. Shin, G. Balas, and A.M. Kaya, *Blending Approach of Linear Parameter Varying Control Synthesis for F-16 Aircraft*, in AIAA Guidance, Navigation and Control Conference, AIAA-01-4040, Montreal, Canada, Aug. 2001, American Institute of Aeronautics and Astronautics.

[10] L. Lee, *Identification and Robust Control of Linear Parameter-Varying Systems*, PhD thesis, Department of Mechanical Engineering, University of California, Berkeley, 1997.

[11] P. Apkarian and R. Adams, *Advanced Gain-Scheduling Techniques for Uncertain Systems*, IEEE Transactions on Control Systems Technology, 6 (1998), pp. 21–32.

[12] P. Gahinet, A. Nemirovski, A. Laub, and M. Chilali, *LMI Control Toolbox*, The Mathworks, Natick, MA, 1995.

[13] R.A. Nichols, R.T. Reichert, and W. Rugh, *Gain Scheduling for $\mathcal{H}_\infty$ Controllers: A Flight Control Example*, IEEE Transactions on Control Systems Technology, (1993), pp. 69–78.

[14] S. Boyd, El. Ghaoui, E. Feron, and V. Balakrisnan, *Linear Matrix Inequalities in System and Control Theory*, Society for Industrial and Applied Mathematics, Philadelphia, PA, 1994.

[15] W. Tan, *Applications of Linear Parameter-Varying Control Theory*, master's thesis, Department of Mechanical Engineering, University of California at Berkeley, 1997.

[16] W. Tan, A. Packard, and G. Balas, *Quasi-LPV Modeling and LPV Control of a Generic Missile*, in Proceedings of the American Control Conference, Chicago, IL, 2000, pp. 3692–3696.

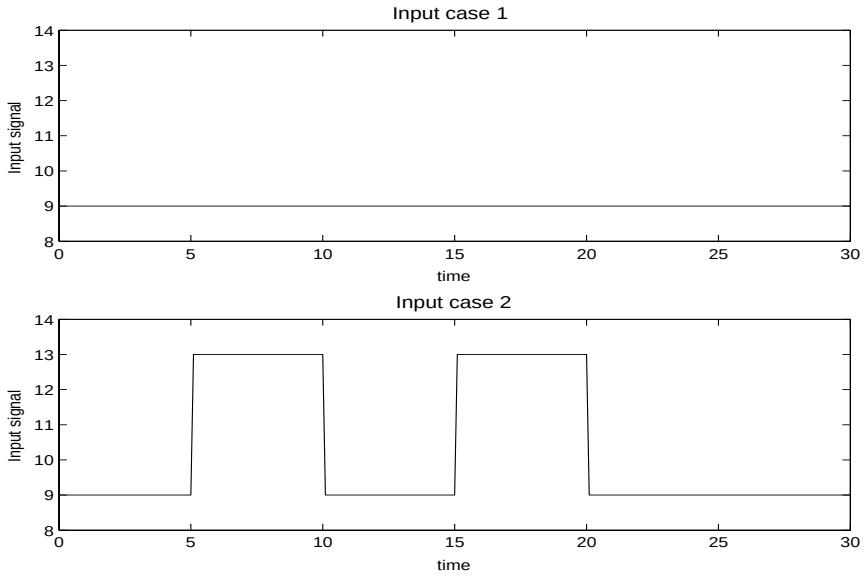

Fig. 5.1. *Input signals.*

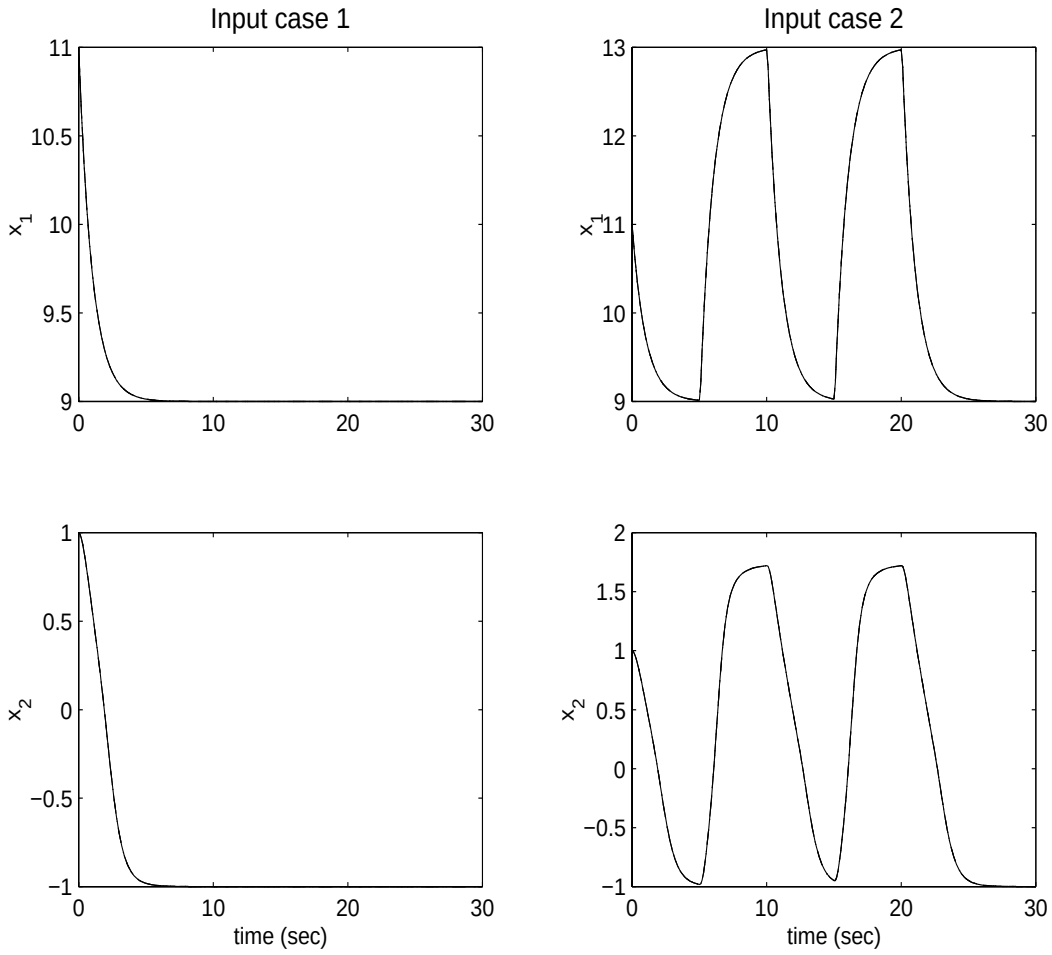

FIG. 5.2. *Quasi-LPV model simulations at two input cases.*

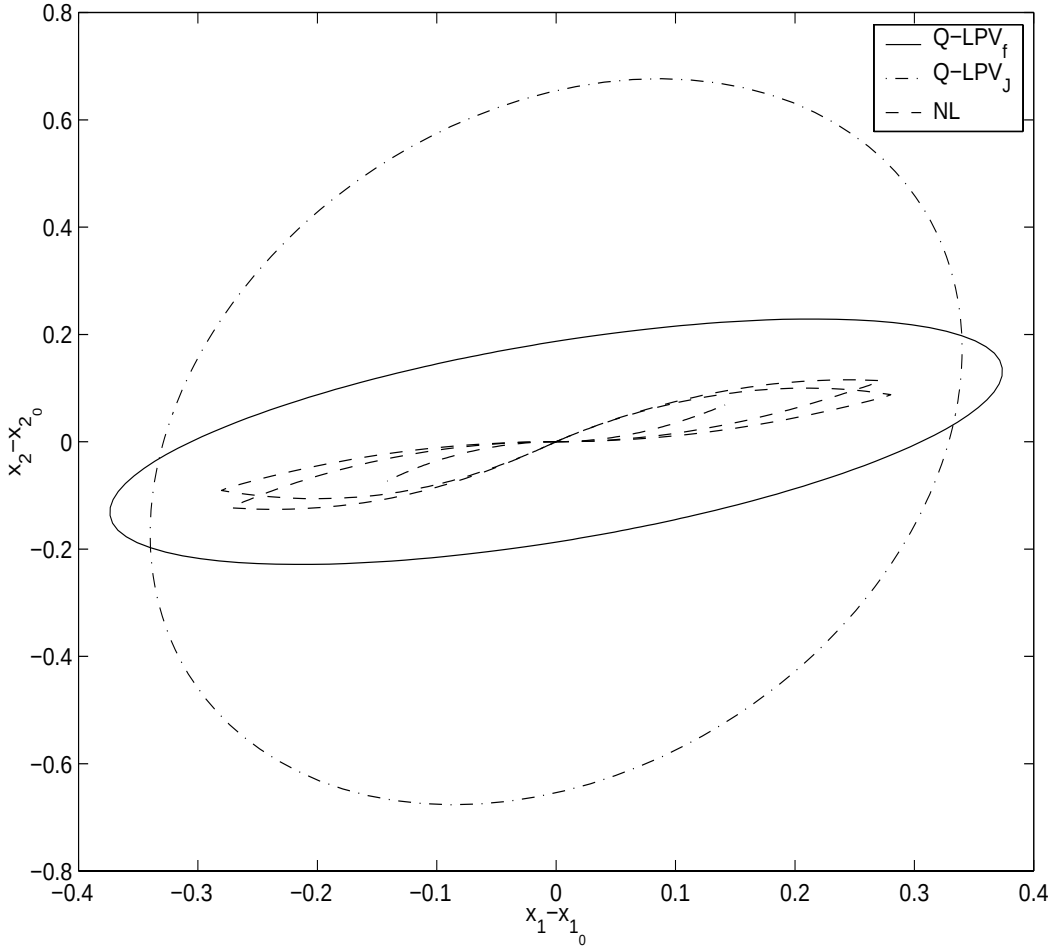

FIG. 5.3. *The ellipsoids to contain a reachable set of the nonlinear dynamics.*

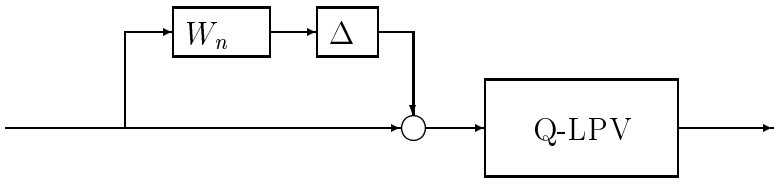

FIG. 5.4. *Quasi-LPV model with unmodeled dynamics*

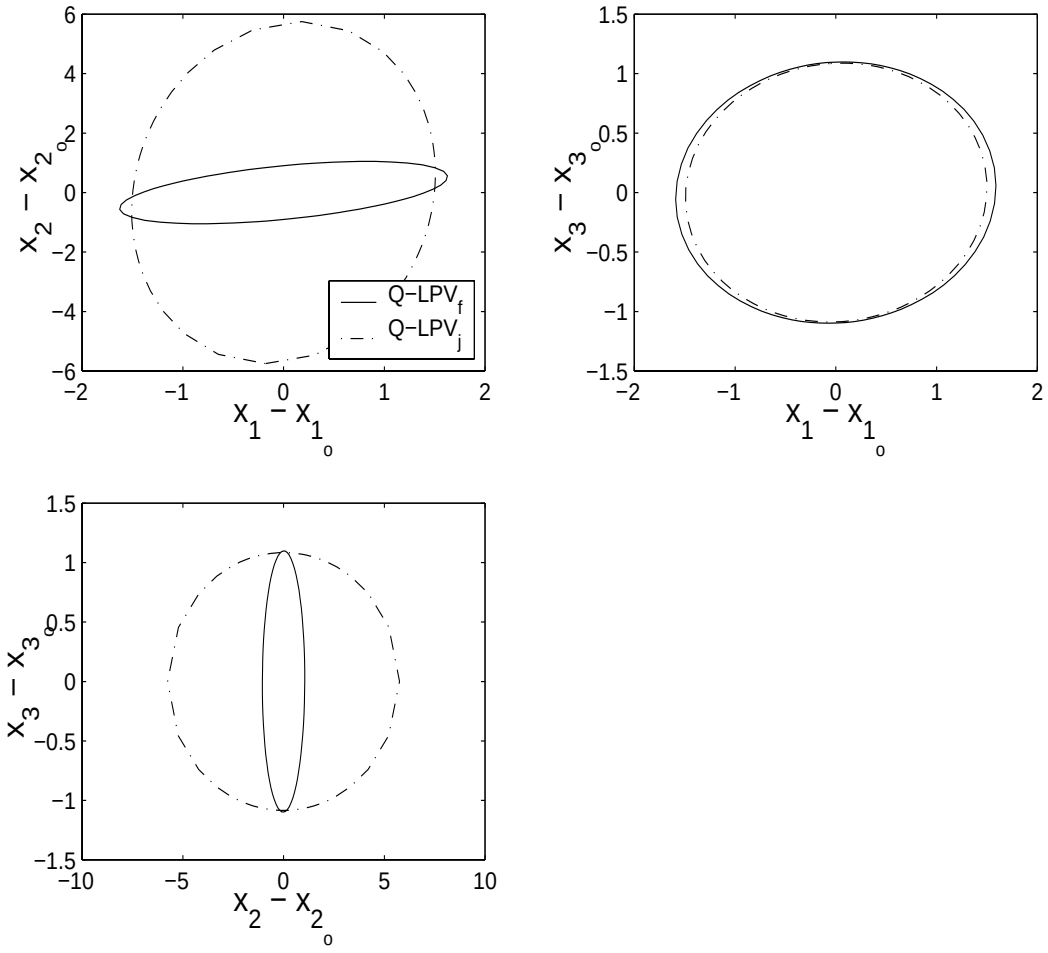

FIG. 5.5. *The ellipsoids based on each quasi-LPV model with unmodeled dynamics.*

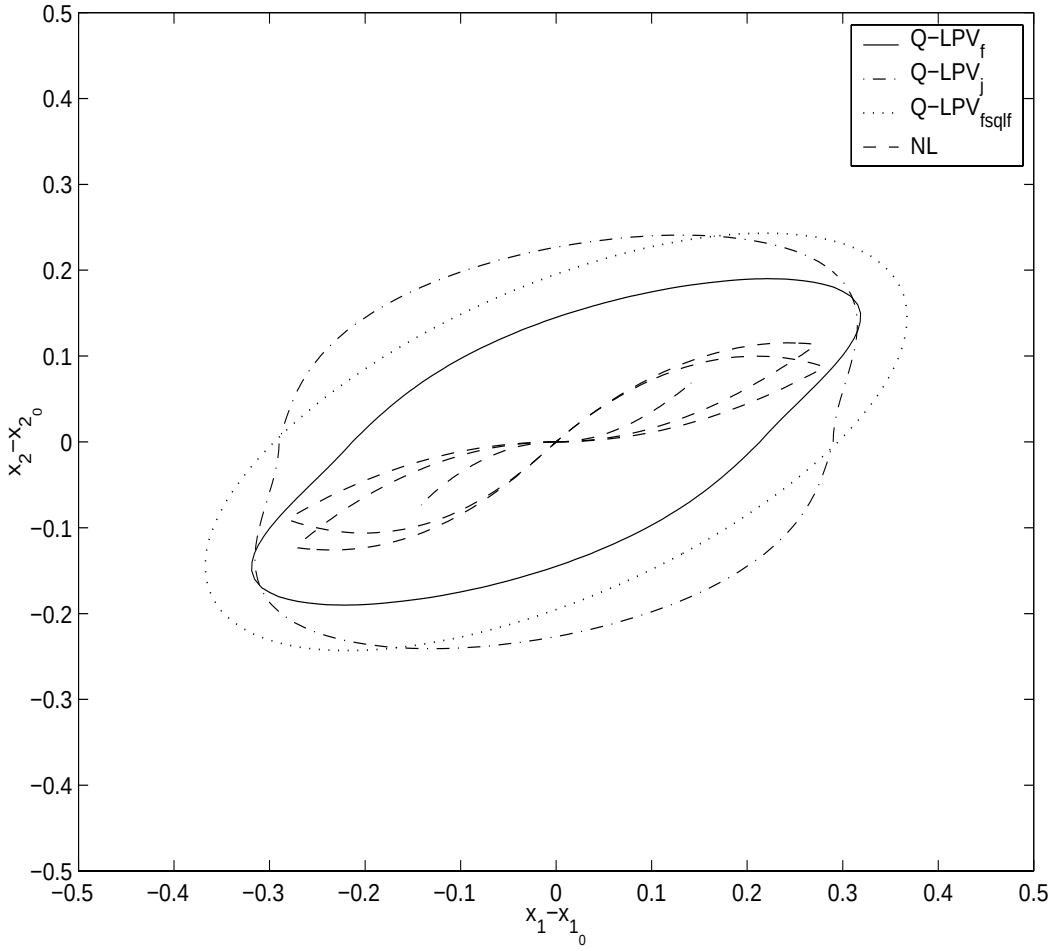

FIG. 5.6. *The set to contain the reachable set* $\mathcal{R}_{bu}$.

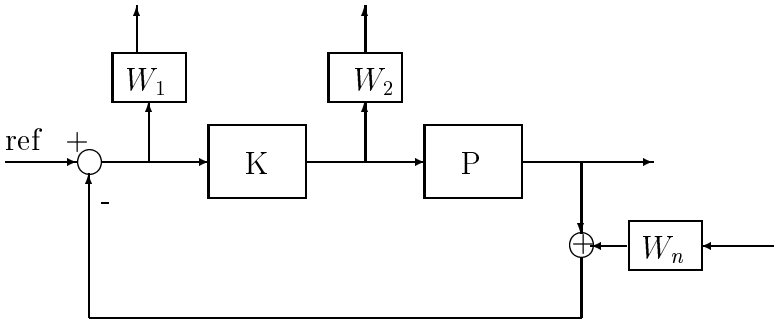

FIG. 5.7. *Interconnection of LPV control synthesis*

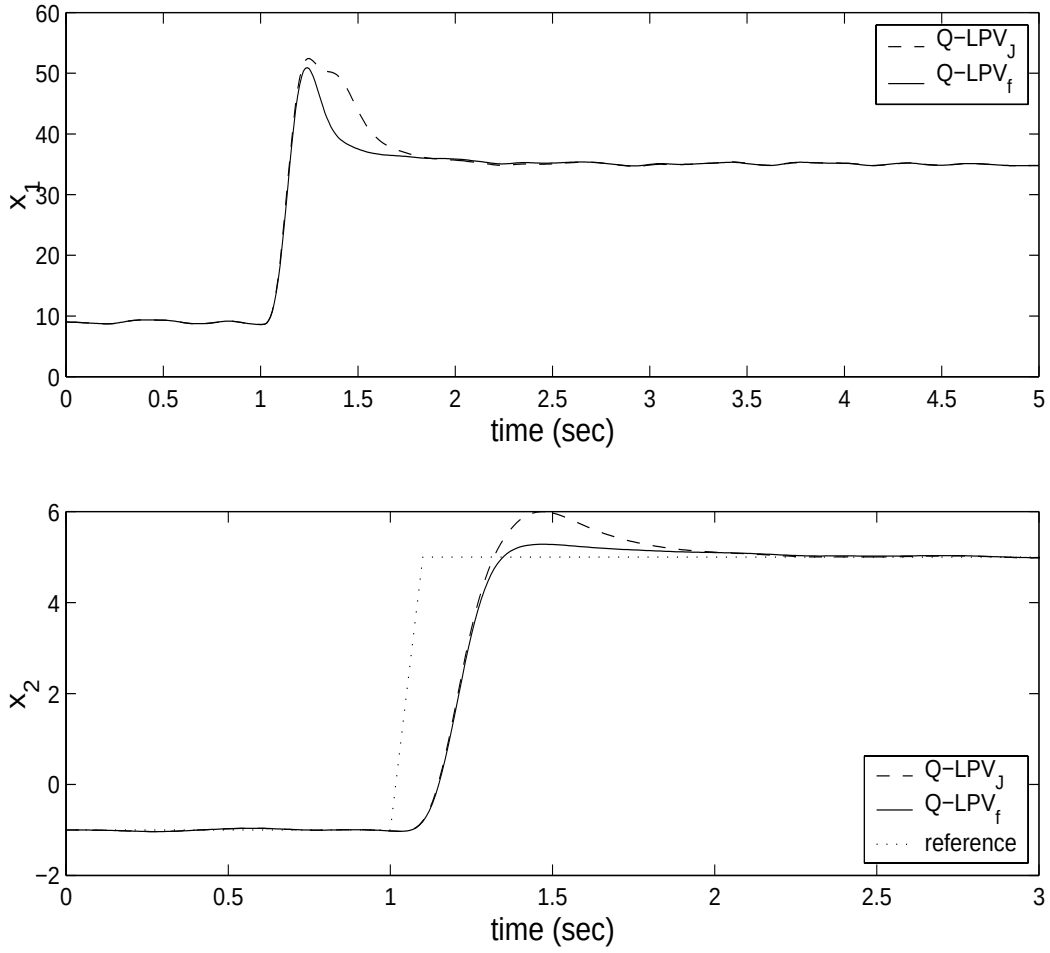

FIG. 5.8. *The step responses based on different quasi-LPV models.*